Journal of Applied Mechanics and Technical Physics, Vol. 41, No. 1, 2000

THERMOHYDRODYNAMICS OF CONTINUOUS-WAVE CO_2 LASERS WITH A CLOSED CYCLE OF THE FLOW

A. I. Ivanchenko, A. M. Orishich, and S. S. Vorontsov

UDC 621.375.826; 621.378.33

The problem of pressure losses upon gas motion along a closed circuit containing channels in which heat is supplied to and removed from the gas is studied. The object where the pressure losses are studied is a CO_2 laser with a crossflow.

With increasing power of electric-discharge lasers with a closed cycle of the flow, the role of the gas-dynamic circuit becomes more important. The gas-dynamic circuit of a powerful continuous-wave CO_2 laser with a crossflow and transverse discharge resembles a subsonic wind tunnel with a closed circuit but differs from the latter by configuration of the gas-discharge chamber wherein the electric energy is converted to radiation and thermal energy.

There are different approaches to designing the gas-dynamic circuit of the laser, and the choice of its schemes is based on contradictory criteria. The circuit has either a large specific volume (3 m^3 per 1 kW of generated power) and a low specific power for sustaining gas circulation over the closed circuit (1 kW per 1 kW) or a high (up to 2 kW per 1 kW) specific power and a comparatively small (1–1.5 m^3 kW) specific volume [1–6]. Various approaches, which are often incompatible, are proposed to choose the pumping tools that ensure gas circulation over a closed circuit and aerodynamic schemes of gas-discharge channels wherein the pumping of the laser mixture of gases is performed. The results of papers devoted to the problem of calculation of pressure losses upon nonisothermal gas flow are contradictory. In the case of nonisothermal motion of gases, the motion becomes nonuniform because of changes in gas densities and, hence, their velocities. This involves pressure losses for gas acceleration [7–10]. Another contradiction arises in calculating the drag of the gas motion over the circuit as a whole. For example, Ivanchenko et al. [4] showed that the cross-sectional area of the flow in a channel where the heat is removed is significantly greater than the cross-sectional area of the flow in a channel with heat addition; therefore, the effect of nonisothermality on the coefficient of pressure losses in a channel with heat removal can be ignored. At the same time, heat addition in real devices does not seem to be inevitably accompanied by pressure losses. For example, Bartlma [9] considered the channel with heat addition as a thermal confuser.

In the present paper, we study the problem of pressure losses upon circulation of a subsonic gas flow over the circuit of a device with a closed cycle, which contains channels wherein heat is supplied to and removed from the gas. The pressure losses are studied in a CO_2 laser with a crossflow. Here and in what follows, the pressure losses are understood as the total (stagnation) pressure losses, which determine the power necessary for gas pumping (see, for example, [8–13]). Nonisothermal motion is understood as a gas flow under conditions of changing stagnation temperature of the flow due to heat addition or removal. The effect of nonisothermality on pressure losses should be understood as the account of additional losses for gas acceleration upon heat addition (removal).

Institute of Theoretical and Applied Mechanics, Siberian Division, Russian Academy of Sciences, 630090 Novosibirsk. Translated from Prikladnaya Mekhanika i Tekhnicheskaya Fizika, Vol. 41, No. 1, pp. 3–13, January–February, 2000. Original article submitted July 16, 1998; revision submitted October 12, 1998.

0021-8944/00/4101-0001 $25.00

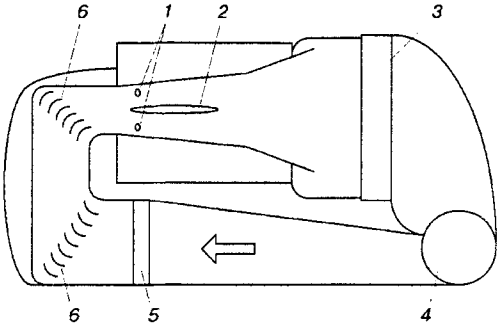

Fig. 1. Layout of the gas-dynamic circuit of a CO_2 laser with a transverse discharge based on a two-module electric-discharge device: 1) cathodes; 2) anodes; 3) heat exchanger; 4) fan; 5) resistance (heat exchanger); 6) rotating blades.

1. Thermohydrodynamics of a Laser with a Closed Cycle of the Flow. One of the possible configurations of the gas-dynamic laser circuit is shown in Fig. 1. The velocity vector of the flow in the gas-discharge chamber is directed perpendicular to the propagation of the laser beam and the discharge current, which decreases the Mach number necessary for changing the gas in the chamber [14]. The flow velocity at the forefront of the gas-discharge channel is usually less than 60–70 m/sec [1–6].

We consider a laser circuit that contains a gas-discharge channel, a heat exchanger, and a fan. The gas-discharge channel and the heat exchanger in which the gas consecutively flows work as a load for the fan. The fan produces a pressure necessary to overcome the drag of gas motion.

The gas-discharge channel is usually a constant-area channel or a two-dimensional diffuser with expansion angles of 7–8°. Gas-flow regimes in these channels correspond usually to Reynolds numbers determined from the hydraulic diameter; the order of magnitude of these Reynolds numbers is $\mathrm{Re} \approx (4\text{–}20)\cdot 10^3$. The total pressure losses for overcoming the friction forces are less than 10% of the losses needed for gas acceleration. In the absence of friction forces, the process in the gas-discharge channel can be described using a system of equations for a plane channel with heat addition [7, 9, 10]

$$\delta(\rho v) = 0, \qquad \delta(p + \rho v^2) = 0, \qquad \delta[v^2/2 + c_p p/((c_p - c_v)\rho)] = \delta q,$$

where ρ is the density, v is the velocity, p is the static pressure, and δq is the heat transferred to a unit mass of the gas. The change in the static temperature of the gas δT is a quantity of the order of the temperature at the entrance T_0. We consider a subsonic flow where $(v/c_s) \ll 1$ (c_s is the speed of sound). The gas is assumed to be in thermal equilibrium. This is justified, since several processes occur simultaneously in the gas-discharge channel: pumping of energy to the upper laser levels, energy extraction with efficiency up to 10–15%, and energy transfer to the lower levels and translational degrees of freedom of molecules.

We make the following assumptions. The gas flow over the circuit is sustained by an isentropic fan. The processes of gas exhaustion from the fan to the gas-discharge channel, from the gas-discharge channel to the heat exchanger, and then to the fan are isentropic. The gas-discharge channel wherein the heat is released is plane and has a constant cross section. The losses for friction in the gas-discharge channels are ignored.

Because of heat release, the stagnation pressure changes by δp_{*q} as the gas passes through the gas-discharge channel. In the heat exchanger, the stagnation pressure changes by δp_{*Q} due to heat removal and by Δp_* due to hydromechanical pressure losses (mainly on overcoming the friction forces). The fan compensates the pressure losses in the circuit. When the gas passes over the closed circuit, its temperature and entropy are unchanged.

Within the framework of these assumptions, the following equalities are valid:

$$\delta p_{*\mathrm{f}} = \delta p_{*q} + \delta p_{*Q}, \qquad \delta T_{*q} + \delta T_{*Q} + \delta T_{*\mathrm{f}} = 0, \qquad \delta s_q + \Delta s_Q = 0. \tag{1}$$

Here and in what follows, the asterisk means that the quantity refers to stagnation parameters, $\delta p_{*\mathrm{f}}$ is the

pressure change in the fan, δT_{*q}, δT_{*Q}, and $\delta T_{*\mathrm{f}}$ are the changes in the gas temperature in passing over the gas-discharge channel, heat exchanger, and fan, respectively, and δs_q and δs_Q are the changes in entropy per unit mass in the gas flow passing through the gas-discharge channel and heat exchanger, respectively. Taking into account Eq. (1), we calculate the pressure losses.

We introduce the following notation. Upstream of the gas-discharge channel, the gas flow has the parameters ρ_0, ρ_{*0}, v_0, p_0, p_{*0}, T_0, and T_{*0}, which are the density, velocity, pressure, and temperature, respectively. At the exit of the gas-discharge channel, the flow parameters are ρ_*, p_*, and T_*.

In the one-dimensional approximation, the processes in the gas-discharge channel and in the heat exchanger can be described using the law of energy conservation $\delta q = \delta h + \delta(v^2/2)$ and the thermodynamic relation

$$T\delta s_q = \delta h - \delta p/\rho, \tag{2}$$

where T is the thermodynamic temperature.

Relation (2) can be written in terms of stagnation parameters:

$$\delta s_q = \delta q/T_* - R(\delta p_{*q}/p_*). \tag{3}$$

In (2) and (3), δq is the energy transferred to a unit mass of the gas flow, δh is the change in enthalpy of a unit mass of the gas flow, T_* is the stagnation temperature, and R is the gas constant, $\mathrm{J/(kg \cdot K)}$.

For a constant-area channel, in the absence of hydromechanical pressure losses caused by friction, relation (2) can be transformed to [9, 10]

$$\delta s_q = \delta q/T. \tag{4}$$

From (3) and (4), we obtain $R(\delta p_{*q}/p_*) = (T_*^{-1} - T^{-1})\delta q$.

Relation (3) can be written in the integral form as

$$\delta s_q = \int\limits_{T_{*0}}^{T_*} c_p \frac{dT_*}{T_*} - \int\limits_{p_{*0}}^{p_*} R\frac{dp_*}{p_*}. \tag{5}$$

In the heat exchanger, the flow parameters change from the values p_* and T_* at the entrance to $p_{*0} - \Delta p_*$ and $T_* - \delta T_{*\mathrm{f}}$ at the exit, and the change in entropy per unit mass of the flow can be presented as

$$\delta s_Q = \int\limits_{T_*}^{T_{*0}-\delta T_{*\mathrm{f}}} c_p \frac{dT_*}{T_*} - \int\limits_{p_{*0}}^{p_{*0}-\Delta p_*} R\frac{dp_*}{p_*}. \tag{6}$$

From relations (1), (5), and (6), it follows that

$$\int\limits_{T_*}^{T_*-\delta T_{*\mathrm{f}}} c_p \frac{dT_*}{T_*} - \int\limits_{p_{*0}}^{p_{*0}-\Delta p_*} R\frac{dp_*}{p_*} = 0, \qquad \delta p_{*\mathrm{f}} = \Delta p_*. \tag{7}$$

It is known that the overall pressure losses in lasers with a transverse discharge are usually a small fraction of the total pressure, and we can assume $\Delta p_*/p_* \ll 1$. To describe the processes in the fan, we can assume that the gas density ρ is constant. With accuracy to the term $\delta T_{*\mathrm{f}}/T_*$, expression (7) can be written in the form

$$\Delta p_*/\rho_* \approx c_p \delta T_{*\mathrm{f}}. \tag{8}$$

From (8), we obtain the expression for the power at the drive of the isentropic fan

$$N \approx V'\Delta p_* \approx \rho V' c_p \delta T_{*\mathrm{f}}.$$

Here, V' is the volume velocity of the gas flow.

The increase in temperature ensured by the isentropic fan can be represented as

$$\delta T_{*\mathrm{f}} = [(1 + \Delta p_*/p_{*-})^{1-(1/\gamma)} - 1]T_{*-}, \tag{9}$$

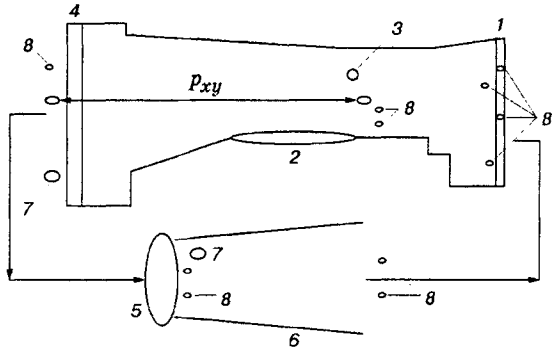

Fig. 2. Layout of experimental facility: 1) grid; 2) anode; 3) cathode; 4) heat exchanger; 5) fan; 6) diffuser; 7) thermometers; 8) pressure probes; the arrows indicate the gas flow direction.

where p_{*-} and T_{*-} are the gas pressure and temperature at the heat-exchanger exit and γ is the ratio of specific heats.

Thus, in devices with a closed circuit, the nonisothermal motion of the gas does not contribute to the overall pressure losses. A decrease in stagnation pressure in the channel with heat addition occurs simultaneously with an equal increase in stagnation pressure in the channel with heat removal. From the viewpoint of gas dynamics, this result is not unexpected. The gas-dynamic circuit can be regarded as a subsonic straight-flow engine with a closed cycle of the flow. Using results of Chernyi [15] who calculated a straight-flow engine, we can show that the pressure losses in the circuit induced by nonisothermal processes are described by the relation $\delta p_* = (\rho_0 v_0^2/2)(1 - \sqrt{1 + (q - Q)/(c_p T_{*0})})$, where q and Q are the amounts of heat per unit mass of the gas flow supplied to the gas and removed from it, respectively. If the total added heat equals zero, the losses due to nonisothermal motion are also equal to zero.

Hydromechanical pressure losses, no matter what their reason is (friction, reconstruction of the flow velocity profile, or constriction and expansion of the flow), are adiabatic processes and do not lead to a local increase in stagnation temperature of the gas flow [10]. An increase in entropy due to hydromechanical losses is compensated by its decrease due to removal of the excess heat by the heat exchanger. The fan performs mechanical work, compensates for inevitable pressure losses, and increases the gas temperature in an isentropic process of gas compression.

2. Experiment. To verify the calculation results, we measured the difference in the total pressures p_{xy} on a "load" containing channels wherein the heat is added and removed, for a constant fan capacity $\rho V'$, in two regimes: with heat addition and without it. This load in the gas-dynamic circuit of the laser is the section between the gas-discharge channel entrance and the heat-exchanger exit. Heat addition was ensured by a glow discharge. The discharge power was sufficient for the total pressure losses in the gas-discharge channel to be $(0.2–0.4)\rho_0 v_0^2$. Good homogeneity of the flow upstream of the gas-discharge channel entrance and a significant difference in cross-sectional areas upstream of the gas-discharge channel and behind the heat exchanger ensured correct measurements.

The experiments were conducted in the gas-dynamic circuit of the laser described in [3–6]. The layout of the experimental setup is shown in Fig. 2. The cross section of the gas path from the region ahead of the gas-discharge channel to the heat-exchanger exit and other elements of the circuit are shown conventionally (not to scale). The path width is 0.93 m. Grid 1, a gas-discharge channel containing anode 2 and cathode 3, and heat exchanger 4 are consecutively placed along the gas flow. The gap between the anode surface and the channel wall is 0.1 m. The characteristic length of the anode in the streamwise direction is 0.12 m. A cylindrical cathode 0.016 m in diameter is placed at a distance of 0.065 m from the anode. In the crossflow direction, the cathode and anode have a length of 0.86 m. The heat exchanger, 0.28 m high, is connected with the gas-discharge channel by a stepwise diffuser. A smooth expansion section begins immediately after the anode, the expansion angle is 12°, and the degree of expansion is 2. The section from the grid to the

anode is constricting, and the degree of constriction is 2. The profile of the section was chosen so that the flows behind the anode were mainly nonseparated or separated depending on test conditions. Behind the heat exchanger, there was fan 5 with diffuser 6 at the exit. Thermometers 7 were located behind the heat exchanger and the fan. Probes of static and total pressure 8 were located in flow cross sections where physical conditions allowed it.

The discharge was ignited in the air flow at a pressure of 10.3 and 16 GPa or in a mixture of CO_2 and air with a ratio 2.66 : 13.3 GPa and 2.66 : 16 GPa. The gas-flow velocity at the forefront of the gas-discharge channel was 60–70 m/sec. The velocity inhomogeneity over the channel cross section did not exceed 3%. The calculated pressure losses in the heat exchanger were about $0.6\rho_0 v_0^2$ in the regime without the discharge and less than $1.1\rho_0 v_0^2$ with the discharge. A variant of calculation of the heat exchanger is shown below. The calculated values of pressure losses at the section between the aft front of the discharge and the heat-exchanger entrance were about $0.2\rho_0 v_0^2/2$. The error in determining the value of p_{xy} was less than $0.1\rho_0 v_0^2/2$.

Primary attention was paid to the measurement of the difference in total pressures p_{xy} on the load using pressure probes mounted upstream of the gas-discharge channel and directly behind the heat exchanger (Fig. 2). The fan capacity was controlled by total and static pressure probes located upstream of the gas-discharge channel. The increase in temperature ensured by the fan allowed us also to control the change in flow regimes at different sections of the circuit. For example, if the height of the heat exchanger was reduced by one quarter, the temperature produced by the fan increased by a factor of 1.4. Additional control of the gas-flow regimes was performed by total and static pressure probes mounted at various points of the circuit.

For the case of a nonseparated flow in the diffuser behind the gas-discharge channel, the experiments gave the following results.

1. The dynamic pressure at the forefront of the gas-discharge channel was $\rho_0 v_0^2/2 \approx p_0 \cdot 2.5 \cdot 10^{-2}$, which corresponds to a mean velocity of the gas $v_0 \approx 65$ m/sec.

2. The fan increased the gas temperature by the same value regardless of the pressure, for example, by 13.6°C for air.

3. The fan capacity in both regimes (with and without the discharge) was constant.

4. The difference in temperature between the gas exhausting from the heat exchanger and the water entering the heat exchanger was not greater than 12–13°C.

5. In both regimes (with and without the discharge), the pressure losses on the load p_{xy} were roughly equal to $0.9\rho_0 v_0^2$.

It should be noted that the experiments with air and laser mixtures gave identical results. From the experiment and thermodynamic calculation, we can conclude that nonisothermal processes do not introduce additional pressure losses for maintaining gas circulation over the circuit.

The absence of the effect of nonisothermality does not mean that heat addition should not be accompanied by an increase in pressure losses. Heat addition increases the mean temperature of the gas, hence, the physical parameters of the flow change, which should lead to an increase in pressure losses, for example, for overcoming the friction forces in the heat exchanger. The calculation of the heat exchanger is explained below. It was expected that heat addition will give an increase in pressure losses by $(0.3\text{–}0.5)\rho_0 v_0^2$. An unexpected result of these experiments was that heat addition was not accompanied by an increase in pressure losses.

A set of experiments on gas-flow visualization was conducted. It was performed using light filaments attached to the surface of the lower wall of the diffuser and the anode surface in a staggered order. The glowing of the anode surface was inhomogeneous. It clearly reflected the flow pattern near the surface. The discharge glowing on the cathode surface was visually homogeneous.

The results of these experiments allowed the following conclusions. The flow in the diffuser behind the anode is three-dimensional. There are vortex regions on the diffuser walls. The vortices rotate in the plane of the wall and are located symmetrically relative to the side walls. A typical size of the vortices is 0.03–0.07 m. The area of the surface occupied by the vortices increases with decreasing velocity and pressure of the gas. When the discharge is ignited, the flow is reconstructed: it becomes more stable, the regions with separated

flows become smaller, and large vortices are split into smaller ones.

Depending on the path configuration ahead of the anode (stepwise entrance, constriction, straightening section, etc.), flow reconstruction occurred; in particular, globally separated flows were observed. In each experiment with air or laser mixtures of gases, the discharge reconstructed the flow pattern, but the value of p_{xy} in both regimes (with and without the discharge) was identical. The reconstruction of flow regimes may be responsible for the fact that heat addition is not accompanied by an increase in pressure losses on the load.

3. Heat Exchanger. We consider an example of calculation of the heat exchanger in the laser circuit. We calculate the heat exchanger with a constant-area plane channel used in our experiments. The calculation is performed using the technique and relations given in [8, 11–13]. The effect of temperature variation is taken into account by the fact that all the calculated parameters are determined for the mean temperature of the gas. The main losses in the heat exchanger are the losses spent on overcoming the friction forces. The flow regimes correspond to $\mathrm{Re} \ll 2000$. The conditions of stabilization of heat-transfer intensity are satisfied. In terms of the gas-flow parameters at the entrance to the gas-discharge channel, the pressure losses on overcoming the friction forces for a steady regime can be described by the equation

$$\xi_0 \gg \zeta\Big(\frac{f_0}{f}\Big)^2\Big(1+\frac{\langle\Delta T_*\rangle}{T_{*-}}\Big), \tag{10}$$

where ξ_0 is the friction coefficient reduced to physical conditions at the entrance to the gas-discharge channel, $\zeta = (96/\mathrm{Re})(L/D)$, L is the channel length, D is the hydraulic diameter, f_0 and f are the cross-sectional areas of the flows in the gas-discharge channel and heat exchanger, respectively, $\langle\Delta T_*\rangle = V'\rho c_p(T_* - T_{*-})/(\Phi F\alpha)$ is the averaged temperature factor of the gas, $\Phi = 0.9$–0.8 is the heat-transfer efficiency, F is the heat-exchange surface of the gas, $\alpha \approx 8\lambda/D$ is the heat-transfer coefficient, and λ is the thermal conductivity. The angular brackets denote the mean value.

At the same time, the quantity ξ_0 is expressed through the temperature difference between the gas and water entering the heat exchanger:

$$\xi_0 = 3\Big(\frac{f_0}{f}\Big)^2\Big(1+\frac{\langle\Delta T_*\rangle}{T_{*-}}\Big)\frac{\mathrm{Pr}}{\Phi}\ln\Big(\frac{T_* - T_{*-}}{\Delta T_{*-}}+1\Big), \tag{11}$$

Here Pr is the Prandtl number and ΔT_{*-} is the temperature factor of the outgoing gas relative to the incoming liquid

$$\Delta T_{*-} = (T_* - T_{*-})(\varepsilon^{-1} - 1); \tag{12}$$

and ε is the heat-exchanger efficiency, which can be expressed by the formula

$$\varepsilon \approx \Big[1-\exp\Big(\frac{\Phi\zeta}{3\mathrm{Pr}}\Big)\exp\Big(\frac{\Phi\zeta}{3\mathrm{Pr}}\frac{\Delta T_{\mathrm{liq}}}{\Delta T_{*Q}}\Big)\Big]\Big[1-\frac{\Delta T_{\mathrm{liq}}}{\Delta T_{*Q}}\exp\Big(-\frac{\Phi\zeta}{3\mathrm{Pr}}\Big)\exp\Big(\frac{\Phi\zeta}{3\mathrm{Pr}}\frac{\Delta T_{\mathrm{liq}}}{\Delta T_{*Q}}\Big)\Big]. \tag{13}$$

where $\Delta T_{*Q} = T_* - T_{*-}$, ΔT_{liq} is the change in the temperature of the cooling liquid passing through the heat exchanger.

The pressure losses Δp_* can be expressed by formula (10) or (11). In contrast to (10), all the quantities of the right part of (11) are determined experimentally. For experimental conditions, the calculations by formulas (10) and (11) coincided within 15% both in regimes with and without the discharge. For these test conditions, the calculations give the following results. In the regime without the discharge, we have $\delta T_{*\mathrm{f}} = T_* - T_{*-} \approx 13.6$ K, $\Delta T_{*-} \approx 2$ K, $(f_0/f)^2 \approx 5$, and $\xi_0 \approx 1.2$. For the ignited discharge, we obtain $T_* - T_{*-} \approx 200$ K, $\Delta T_{*-} \approx 12$ K, $1 + \langle\Delta T_*\rangle/T_{*-} \approx 1.2$, and $\xi_0 \approx 1.9$. A combination of the parameters that enter the right part of Eq. (11) allows one to determine the drag coefficient on the basis of experimental data on the thermal characteristics of the heat exchanger:

$$\zeta = 3\frac{\mathrm{Pr}}{\Phi}\ln\Big(\frac{T_* - T_{*-}}{\Delta T_{*-}}+1\Big).$$

Substituting the obtained value of ζ into (13), we calculate the heat-exchanger efficiency and then the temperature factor ΔT_{*-} using formula (12). The resultant value of ΔT_{*-} coincides with the initial one within

20%. The calculation accuracy for ξ_0 depends on the error f_0/f, where f is determined from the experiment within 15% (the heat exchanger experiences the action of a nonuniform flow, and it is difficult to find the exact value of f).

The calculation results for ξ_0 show that the pressure losses increase with increasing difference $(T_* - T_{*-})$. Nevertheless, this was not registered in experiments with measurement of the pressure difference on the load, which is possibly explained by the decrease in pressure losses in the diffuser upstream of the heat exchanger with increasing $(T_* - T_{*-})$.

The accuracy of the numerical model was checked using the gas-dynamic circuit of a laser based on a diameter fan developed at the Institute of Theoretical and Applied Mechanics of the Siberian Division of the Russian Academy of Sciences. In this fan, the diffuser ahead of the heat exchanger is made symmetric with smooth expansion (the total angle of expansion is 8°). The pressure losses in the diffuser can be ignored. The pressure losses on the load calculated by formula (11) or (12) are in good qualitative and quantitative agreement (the error is within 20%) with experimental results.

4. Gas-Dynamic Circuit. Real Pressure Losses. Verification of the basic postulates of the numerical model requires experimental data on aerodynamic characteristics of the laser circuit and its components. However, there are no publications that describe the results of testing gas-dynamic circuits of lasers. These tests present certain difficulties. In particular, an aerodynamic balance should be built into the gas-dynamic circuit to determine the aerodynamic characteristics of the fan. The results of thermodynamic calculations offer a comparatively simple method for determining the aerodynamic characteristics of the gas-dynamic circuit.

From Eq. (8), we can derive the following dependence of the stagnation temperature induced by an isentropic fan on the total pressure losses at the section of the gas path, which contains a section with the fan and does not contain channels with heat addition (removal):

$$\sum_{i=1}^{n} c_p \rho \delta T_{*i} \approx \sum_{i=1}^{n} \delta p_i. \tag{14}$$

The right part of (14) is the sum of the total pressure losses on all sections, including the section with the fan. The assumption of constant density made in (14) is valid if the section does not contain channels with heat addition or removal. Each value of δp_{*i} corresponds to an increase in stagnation temperature δT_{*i} generated by the fan.

From (9) and (14), there follows the relation for the hydraulic efficiency of the gas path with a fan: $\eta \approx \delta T_{*\mathrm{f}}/\delta T_{*p}$, where δT_{*p} is the temperature increase due to a real fan, which is determined experimentally. The calculation by formula (9) is performed in terms of stagnation parameters assuming a uniform flow over the cross-sectional area at the entrance and at the exit. The increase in the total pressure over the section is calculated by the formula $\delta p_* \approx p_- - p_+ + 0.5\rho[\langle v_- \rangle^2 - \langle v_+ \rangle^2]$, where p_- and p_+, $\langle v_- \rangle$ and $\langle v_+ \rangle$ are the values of static pressures and velocities of the gas flow averaged over the cross-sectional areas at the entrance and exit, respectively.

There is almost nothing said about this method in publications devoted to testing of aerodynamic paths of various devices, including lasers, except for [11], where this method was used for testing a fan. The values of η measured by an aerodynamic balance and calculated from the ratio of the temperature difference (14) coincided within 10%.

The gas-dynamic circuit of the laser can be divided into functional sections. The sections should not contain channels wherein heat is supplied, i.e., the total heat addition to each section should be equal to zero. If we find the hydraulic efficiency of the functional sections and the coefficient of pressure losses (drag) of one of the sections, we can calculate the coefficients of pressure losses of other sections and, on the basis of data on flow parameters upstream of the gas-discharge channel, calculate the pressure produced by the fan. Indeed, we divide the circuit into three components: the load (from the entrance to the gas-discharge channel to the heat-exchanger exit), the grid, and the fan, which have the coefficients of pressure losses r_{01}, r_{02}, and r_{03}. Then, the hydraulic efficiency of the circuit determined by the load can be expressed as

$$\eta_x = \frac{r_{01}}{r_{01} + r_{02} + r_{03}},$$

and the hydraulic efficiency of the fan is

$$\eta = \frac{r_{01} + r_{02}}{r_{01} + r_{02} + r_{03}}.$$

The left parts of the equations and the drag coefficient of the load are known. This is sufficient to calculate the values of r_{02} and r_{03}.

The pressure produced by the fan is determined through the drag coefficient of the circuit and the flow parameters at the entrance to the gas-discharge channel:

$$\delta p_{*\mathrm{f}} = \zeta_0 \rho_0 v_0^2/2. \tag{15}$$

The value of $\delta p_{*\mathrm{f}}$ is determined from the formula [11, 16]

$$\delta p_{*\mathrm{f}} = \Psi \rho u^2/2, \tag{16}$$

where Ψ is the pressure coefficient and u is the circumferential velocity of the wheel of the fan. From (15) and (16), we calculate the pressure coefficient of the fan $\Psi \approx \zeta_0 (v_0/u)^2$.

In our experiments, we obtained the following aerodynamic characteristics of the laser [4]: $r_{01} \approx 1.8$, $r_{02} \approx 1.3$, $r_{03} \approx 2.3$, $\zeta_0 = r_{01} + r_{02} \approx 3.1$, $\Psi \approx 1$, and $\eta \approx 0.57$; the calculated characteristics are $\zeta_0 \approx 2$, $\Psi \approx 1.6$–1.8, and $\eta \approx 0.5$–0.7. The numerical values of Ψ and η are given with account of the Reynolds number effect on them. The calculated values of the characteristics of circuit elements do not coincide with the values obtained experimentally. The reason for this disagreement is that the flows in channels with variable cross sections are separated, which is confirmed experimentally. The values of the pressure losses obtained on the basis of experimental data on the flow characteristics in channel cross sections coincide with those obtained by this method.

The calculations of aerodynamic characteristics of gas-dynamic laser circuits on the basis of diameter and centrifugal fans for the case of nonseparated flows yield satisfactory agreement with experiment. In these calculations, we used the aerodynamic schemes and parameters of fans presented in [16–18].

Conclusion. It follows from thermodynamic calculations and experiments that additional losses of the total pressure for gas acceleration, which occur in the case of nonisothermal gas flow, should not be taken into account for devices with a closed cycle of subsonic flow, which contain channels with heat addition to the gas and heat removal from it. These additional losses do not contribute to the overall pressure losses if the gas passes over a closed circuit. In the case of nonisothermal flow, the hydromechanical losses of the total pressure can be determined by the same method as in an isothermal flow. Only the dependence of the physical parameters of the gas on its temperature is taken into account.

It is shown that heat addition to the channel is not necessarily accompanied by an increase in pressure losses. The physical parameters of the flow change due to heat addition, and the pressure losses should increase. At the same time, heat addition alters the flow structure, which can lead to an increase in pressure losses.

By means of visualization, it was found that the flow in a two-dimensional diffuser can be three-dimensional, which is manifested in formation of large-scale vortices rotating in the plane of the diffuser wall.

The authors are unaware of any publications devoted to the problem of three-dimensional flows in two-dimensional diffusers. In experiments, three-dimensional flows were observed for very small angles of expansion (about 12°). However, there are publications on three-dimensional flows arising in the flow around a wing mounted at a certain angle of attack. Zanin [19] describes the results of experiments conducted in the T-324 low-turbulent wind tunnel based at the Institute of Theoretical and Applied Mechanics of the Siberian Division of the Russian Academy of Sciences. He studied the three-dimensional structure of the flow around a wing and the changes in this structure induced by sequential increasing and decreasing of the flow velocity. The experiments [19] were conducted at an atmospheric pressure for flow velocities of 0–23 m/sec; the model

span was 0.945 m and the chord length was 0.196 m. As a whole, similar flow patterns were observed under test conditions [19] and in our experiments. As in [20], the flow structure under our experimental conditions could be reconstructed by placing steps in the vortex region or by mounting a flap (rotating blade) behind the diffuser near its wall. The physical mechanisms of three-dimensional flows and the effect of the discharge on them remain unclear yet.

The authors are thankful to B. Yu. Zanin and V. V. Kozlov who helped in conducting the experiment on visualization of aerodynamic flows and comparison with the wind-tunnel results.

This work was supported by the Russian Foundation for Fundamental Research (Grant No. 98-02-17936).

REFERENCES

1. G. A. Abil'siitov, V. S. Golubev, and F. V. Lebedev, "Problems of creation of industrial technological lasers with power 1–10 kW." *Izv. Akad. Nauk SSSR, Ser. Fiz.*, **47**. No. 8, 1507–1512 (1983).
2. G. A. Abil'siitov, E. P. Velikhov, V. S. Golubev, et al., *Powerful Gas-Discharge CO_2 Lasers and Their Application in Technology* [in Russian], Nauka, Moscow (1984).
3. A. I. Ivanchenko, V. V. Krasheninnikov, A. G. Ponomarenko, and A. A.Shepelenko, "Compact radiator of a technological CO_2 laser," *Kvant. Élektron.*, **12**, No. 10, 2155–2156 (1985).
4. A. I. Ivanchenko, V. V. Krasheninnikov, A. G. Ponomarenko, and A. A. Shepelenko, "Selecting gas-dynamic channel parameters for electrical discharge fast flowrate lasers," *Prikl. Mekh. Tekh. Fiz.*, **27**, No. 6, 3–8 (1986).
5. V. K. Golov, A. I. Ivanchenko, V. V. Krasheninnikov, et al., "Technological CO_2 laser with power 2.5 kW," *Izv. Sib. Otd. Akad. Nauk SSSR, Ser. Tekh. Nauk*, **2**, No. 10, 87–91 (1986).
6. A. I. Ivanchenko, V. V. Krasheninnikov, A. G. Ponomarenko, and A. A. Shepelenko, "Development and creation of technological CO_2 lasers with power 2–5 kW," in: *Application of Lasers in National Economy* [in Russian], Nauka, Moscow (1986), pp. 53–62.
7. A. Hertzberg, W. H. Christiansen, E. W. Johnston, and H. G. Ahlstrom, "Photon generators and engines for laser power transmission." *AIAA J.*, **10**, No. 4, 394–400 (1972).
8. M. A. Mikheev and I. M. Mikheeva, *Fundamentals of Heat Transfer* [in Russian], Energiya, Moscow (1977).
9. F. Bartlma, *Gasdynamik der Verbrennung*, Springer-Verlag, Wien (1975).
10. G. N. Abramovich, *Applied Gas Dynamics* [in Russian], Nauka, Moscow (1986).
11. B. Eck, *Fans; Design and Operation of Centrifugal, Axial-Flow, and Cross-Flow Fans*, Pergamon Press, Oxford–New York (1973).
12. E. R. G. Eckert and R. M. Drake, *Introduction to Heat and Mass Transfer*, McGraw-Hill, New York (1963).
13. I. E. Idel'chik, *Handbook on Hydraulic Resistances* [in Russian], Mashinostroenie, Moscow (1992).
14. P. E. Cassady, "Fluid dynamics in closed-cycle pulsed lasers," *AIAA J.*, **23**, No. 12, 1922–1931 (1985).
15. G. G. Chernyi, *Gas Dynamics* [in Russian], Nauka, Moscow (1988).
16. T. S. Solomakhova and K. V. Chebysheva, *Centrifugal Fans. Aerodynamic Schemes and Characteristics: Handbook* [in Russian], Mashinostroenie, Moscow (1980).
17. A. G. Korovkin, "Investigation of the bodies of diameter fans," *Prom. Aérodin.*, No. 32, 176–189 (1975).
18. A. G. Korovkin and A. N. Feofilaktov, "Parametric investigation of a diameter fan with a high efficiency," *Prom. Aérodin.*, No. 4, 308–326 (1991).
19. B. Yu. Zanin, "Hysteresis of a separated variable-velocity flow about a straight-wing model," *Prikl. Mekh. Tekh. Fiz.*, **38**, No. 5, 80–84 (1997).
20. B. Yu. Zanin, V. V. Kozlov, and O. V. Mavrin, "Method of controlling global separation of the flow," *Teplofiz. Aéromekh.*, **4**, No. 4, 381–385 (1997).